28. I. Gusarov and E. Nudler, *Mol. Cell* **3**, 495 (1999); W. S. Yarnell and J. W. Roberts, *Science* **284**, 611 (1999).
29. S. M. Uptain, C. M. Kane, M. J. Chamberlin, *Annu. Rev. Biochem.* **66**, 117 (1997).
30. S. Borukhov, J. Lee, A. Goldfarb, *J. Biol. Chem.* **266**, 23932 (1991); V. Markovtsov, A. Mustaev, A. Goldfarb, *Proc. Natl. Acad. Sci. U.S.A.* **93**, 3221 (1996); V. Epshtein *et al.*, in preparation.
31. A. Polyakov *et al.*, *J. Mol. Biol.* **281**, 262 (1998).
32. S. A. Darst, A. Polyakov, C. Richter, G. Zhang, *Cold Spring Harbor Symp. Quant. Biol.* **63**, 269 (1998); S. A. Darst, N. Opalka, A. Polyakov, C. Richter, G. Zhang, in preparation.
33. E. Zaychikov *et al.*, *Science* **273**, 107 (1996); A. Mustaev *et al.*, *Proc. Natl. Acad. Sci. U.S.A.* **94**, 6641 (1997).
34. S. Borukhov *et al.*, *J. Biol. Chem.* **266**, 23921 (1991); K. Severinov *et al.*, *J. Biol. Chem.* **269**, 14254 (1994).
35. M. S. Bartlett, T. Gaal, W. Ross, R. L. Gourse, *J. Mol. Biol.* **279**, 331 (1998).
36. J. F. W. Keana and S. X. Cai, *J. Org. Chem.* **55**, 3640 (1990).
37. K. Severinov *et al.*, *Proc. Natl. Acad. Sci. U.S.A.* **92**, 4591 (1995); K. Severinov *et al.*, *J. Biol. Chem.* **271**, 27969 (1996).
38. Figures 3 and 4 were made with the program GRASP [A. Nicholls, K. A. Sharp, B. Honig, *Prot. Struct. Funct. Genet.* **11**, 281 (1991)]. We thank K. Severinov for the strain overproducing the Xho 19 β subunit mutant and M. Chlenov for participation in development of the DNA-protein cross-linking methods. Supported in part by NIH grants GM30717 and GM49242 (to A.G.) and NIH grant GM53759 (to S.A.D.).

3 May 2000; accepted 5 June 2000

Soluble Adenylyl Cyclase as an Evolutionarily Conserved Bicarbonate Sensor

Yanqiu Chen,* Martin J. Cann,*† Tatiana N. Litvin, Vadim Iourgenko, Meeghan L. Sinclair, Lonny R. Levin, Jochen Buck

Spermatozoa undergo a poorly understood activation process induced by bicarbonate and mediated by cyclic adenosine 3′,5′-monophosphate (cAMP). It has been assumed that bicarbonate mediates its effects through changes in intracellular pH or membrane potential; however, we demonstrate here that bicarbonate directly stimulates mammalian soluble adenylyl cyclase (sAC) activity in vivo and in vitro in a pH-independent manner. sAC is most similar to adenylyl cyclases from cyanobacteria, and bicarbonate regulation of cyclase activity is conserved in these early forms of life. sAC is also expressed in other bicarbonate-responsive tissues, which suggests that bicarbonate regulation of cAMP signaling plays a fundamental role in many biological systems.

Ejaculated spermatozoa are not competent to fertilize an egg. They must first undergo a number of bicarbonate-induced processes, including the induction of hyperactivated motility, capacitation, and the acrosome reaction (*1*–*3*). Each of these processes is known to be cAMP-dependent, but they do not appear to involve the widely studied, hormone-responsive, transmembrane adenylyl cyclases (tmACs). We recently described the purification and cloning of a form of mammalian adenylyl cyclase, the sAC, that is structurally, molecularly, and biochemically distinct from the heterotrimeric guanosine triphosphate–binding protein (G protein)–regulated tmACs (*4*). The sAC cDNA encodes a 187-kD protein that is proteolytically processed to the mature 48-kD isoform purified from rat testes (*4*). Regulators of sAC activity have not yet been identified; tmAC modulators such as G proteins and forskolin do not affect sAC activity (*4*–*6*). Because sAC message is most abundantly expressed in male germ cells (*4*, *7*) and its activity is distinct from that of tmACs, we tested whether sAC mediated the bicarbonate-induced cAMP increase in sperm.

Department of Pharmacology, Joan and Sanford I. Weill Medical College of Cornell University, 1300 York Avenue, New York, NY 10021, USA.

*These authors contributed equally to this work.
†To whom correspondence should be addressed.

Western blotting confirmed sAC's presence in bicarbonate-responsive spermatozoa. Anti-sAC antisera (*8*) detected the 48-kD mature form (*4*) and also detected higher molecular weight precursors in both rat testis and mouse epididymal sperm (Fig. 1B). Native sAC was also detected in other tissues known to regulate bicarbonate concentrations and reported to contain bicarbonate-stimulated AC activity (*9*), such as the kidney and the choroid plexus (Fig. 1B). These antisera specifically immunoprecipitated a bicarbonate-stimulated AC activity from the cytosol of rat testis (Fig. 1C) (*10*). The activity was not forskolin-responsive and is therefore unlikely to be caused by cross-reacting tmACs in the immunoprecipitate. Contrary to previous reports in which its in vitro activity required nonphysiologically relevant concentrations of Mn^{2+}–adenosine triphosphate (ATP) (*4*, *11*), sAC activity in these immunoprecipitates was measured in the presence of the more physiologically relevant substrate Mg^{2+}-ATP. These data suggest that sAC is responsible for bicarbonate-stimulated cAMP accumulation in the testis and sperm and that bicarbonate may be acting directly on sAC enzymatic activity.

The effect of bicarbonate on sAC activity was tested in a stable HEK293 cell line expressing the full-length (sAC_{fl}) cDNA (HEK293/sAC_{fl}). Addition of $NaHCO_3$ to the extracellular medium stimulated cAMP accumulation in HEK293/sAC_{fl} cells but not in vector-transfected HEK293 cells (HEK293/V) (Fig. 2A) (*12*). The bicarbonate concentrations used in this experiment mimic the increase observed in sperm (from ≤5 mM in caudal epididymal sperm before ejaculation to ≥25 mM after ejaculation) (*13*). Bicarbonate increased cAMP production within minutes of its addition (*14*), concomitant with an observed elevation of intracellular pH indicating that bicarbonate had entered the cell (*15*). These data demonstrate that sAC can be activated by bicarbonate in a cellular context in the absence of any additional testis- or sperm-specific factors.

To delineate the regions of sAC that mediate bicarbonate activation, we constructed an additional stable cell line (HEK293/sAC_t) expressing a catalytically active NH_2-terminal truncation consisting almost exclusively of the two catalytic domains (sAC_t), which approximates the native 48-kD species (*4*). Bicarbonate also stimulated cAMP accumulation in HEK293/sAC_t cells (*14*), revealing that bicarbonate stimulation of sAC activity does not require the large COOH-terminal domain. Bicarbonate also activated heterologously expressed sAC in vitro. AC activity was stimulated in cellular lysates from HEK293/sAC_{fl} and HEK293/sAC_t cells (Fig. 2B), which is consistent with the idea that the enzyme is directly modulated by bicarbonate ions.

To demonstrate that bicarbonate acts directly on sAC and to exclude the possibility of accessory factors mediating activation in preparations from testis (Fig. 1C) and stable cell lines (Fig. 2), we purified recombinant sAC_t protein (*16*). Purified enzyme was stimulated more than sevenfold (Fig. 3A) with a median effective concentration (EC_{50}) (25.4 ± 7.6 mM) within the physiologically relevant bicarbonate concentration in mammalian serum (22 to 26 mM) (*17*, *18*). Presumably, this direct activation of sAC accounts for the observed intracellular increase in cAMP generation in sAC-expressing cell lines (Fig. 2A).

Bicarbonate stimulation was not due to altered pH, because both Mg^{2+}-ATP alone and bicarbonate-stimulated sAC activities were completely insensitive to pH changes

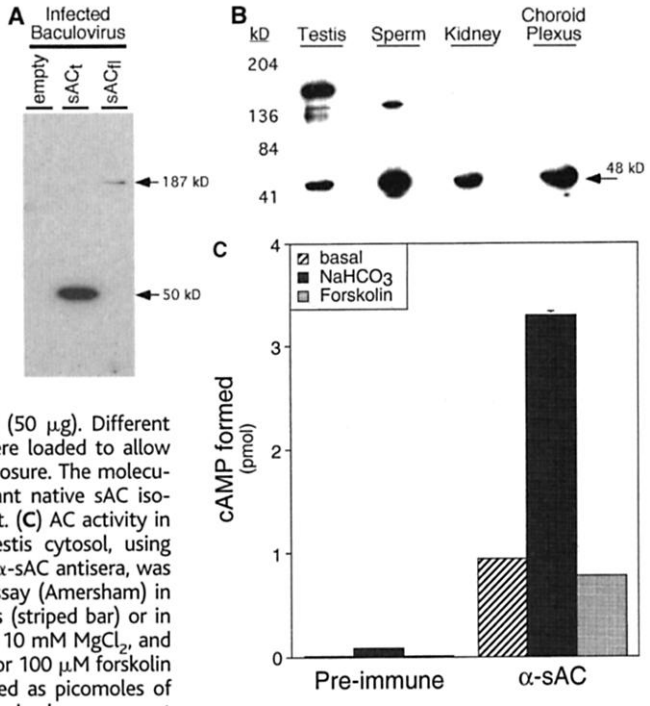

Fig. 1. sAC is present in bicarbonate-sensing tissues. (**A**) Antisera to sAC specifically recognize heterologously expressed sAC protein in HiFive cells infected with recombinant baculoviruses expressing the indicated proteins ("empty" refers to empty baculovirus vector). The predicted sizes of heterologously expressed proteins are indicated on the right. (**B**) Anti-sAC Western blot of the testis (30 μg), sperm (5 μg), kidney (50 μg), and choroid plexus (50 μg). Different amounts of total protein were loaded to allow direct comparison in one exposure. The molecular weight of the predominant native sAC isoform is indicated on the right. (**C**) AC activity in immunoprecipitates from testis cytosol, using either preimmune serum or α-sAC antisera, was measured by radioimmunoassay (Amersham) in the absence of any additions (striped bar) or in the presence of 10 mM ATP, 10 mM $MgCl_2$, and 40 mM $NaHCO_3$ (black bar) or 100 μM forskolin (gray bar). Data are presented as picomoles of cAMP formed over 20 min, and values represent averages of duplicate determinations, with SDs indicated by error bars.

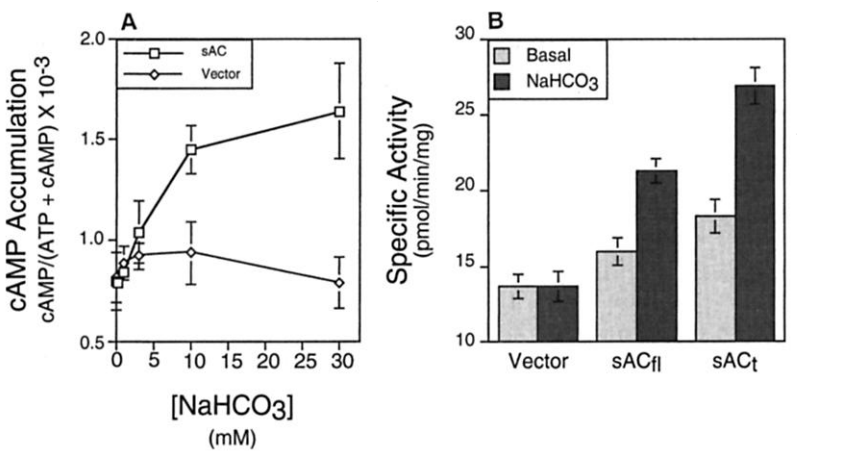

Fig. 2. sAC is stimulated by bicarbonate. (**A**) Cellular cAMP accumulation was measured in stable cell lines expressing expression vector alone (diamonds) or sAC_{fl} (squares) at the indicated concentrations of $NaHCO_3$ after growth for 24 hours in bicarbonate-free medium. Data are expressed as cAMP formed relative to total adenine nucleotides, and values represent averages of quadruplicate determinations with SDs indicated by error bars. (**B**) In vitro cyclase activity (measured in the presence of 5 mM $MgCl_2$) in extracts from stable cell lines expressing empty expression vector, sAC_{fl}, or sAC_t in the presence (dark bars) or absence (light bars) of 50 mM $NaHCO_3$. Data are expressed as picomoles of cAMP formed per minute per milligram of total cellular protein, and values represent averages of triplicate determinations, with SDs indicated by error bars.

over the range 7.0 to 8.5 (Fig. 3B). sAC activity was stimulated equally well by $NaHCO_3$ or $KHCO_3$, and we were able to mimic the stimulatory effects of $NaHCO_3$ using bisulfite ion (Na_2SO_3 or $NaHSO_3$), which structurally resembles bicarbonate, but not with dissimilar ions, such as chloride (NaCl), sulfate (Na_2SO_4), or phosphate (Na_2HPO_4) (Table 1). These data exclude Na^+ ion and simple alterations of ionic strength as regulators of sAC activity, and they indicate that bicarbonate, as opposed to CO_2, directly binds to and activates sAC in a pH-independent manner. However, because carbon dioxide is in equilibrium with bicarbonate, sAC and the cAMP signaling pathway may also indirectly monitor in vivo levels of carbon dioxide.

Among mammalian ACs, sAC appears to be the only form regulated by bicarbonate

Table 1. Activation of sAC by various salts.

Salt*	% Basal†
$NaHSO_3$	138 ± 4.6
Na_2SO_3	164 ± 2.9
NaCl	93 ± 11.8
Na_2HPO_4	75 ± 2.6
Na_2SO_4	66 ± 4.6
$NaHCO_3$	411 ± 5.3
$KHCO_3$	412 ± 6.1

*Salts were used at 50 mM. †AC activity shown relative to activity in the absence of any added salts. The assay included 40 mM $MgCl_2$, 50 mM tris (pH = 7.5), and 10 mM [α^{32}P]ATP (specific activity 6 × 10^3 dpm/nmol). Values used were averages of triplicate determinations and are presented with SDs.

ions. HEK293/V cells, which express endogenous tmACs, are unaffected by the addition of bicarbonate (Fig. 2). Even when submaximally stimulated by forskolin, tmAC activity was insensitive to bicarbonate (*14*). Finally, although a purified, engineered, soluble form of tmAC [type V (*19*)] was fully responsive to forskolin, it was completely insensitive to bicarbonate addition (Fig. 3C). Therefore, bicarbonate stimulation is not a general feature of all ACs, and mammalian cells possess two independently regulated cAMP signal transduction systems.

The two catalytic domains of sAC (C1 and C2) (*4*) more closely resemble the active portions of cyanobacterial ACs than those from mammalian tmACs (Fig. 4A). It has been hypothesized that cyanobacteria (blue-green algae) were the predominant form of life in the carbon dioxide–rich, pre-Cambrian environment (*20*). They are thought to be responsible for the photosynthesis that transformed early Earth's carbon dioxide–rich atmosphere into an oxygen atmosphere (*20*). cAMP is known to regulate respiration in cyanobacteria (*21*), but there is no known molecule that modulates their AC activity. The similarity between sAC and cyanobacterial ACs prompted us to examine whether bicarbonate regulation of cAMP signaling is conserved in cyanobacteria. The AC activity of purified *Spirulina platensis* CyaC was stimulated 2.5-fold by the presence of bicarbonate ions (Fig. 4B). Similar to mammalian sAC, bicarbonate-stimulated cyanobacterial CyaC with an EC_{50} of 18.8 ± 1.6 mM and bicarbonate regulation was pH-independent (*14*). These data demonstrate that cyanobacterial ACs can also serve as bicarbonate sensors and that bicarbonate regulation of AC activity is conserved across phyla separated by hundreds of millions, if not billions, of years.

We have demonstrated that the physiologically ubiquitous ion bicarbonate stimulates the production of a second messenger molecule, cAMP, by direct modulation of enzymatic activity. Our data suggest that sAC is the chemosensor mediating bicarbonate's effects during sperm activation, and they define sAC as a potential target

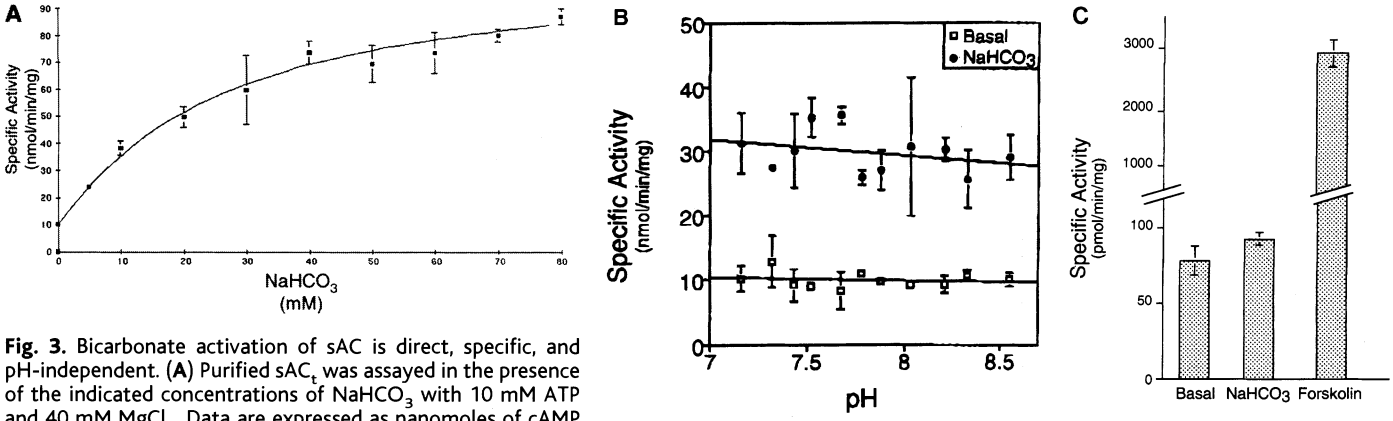

Fig. 3. Bicarbonate activation of sAC is direct, specific, and pH-independent. (**A**) Purified sAC_t was assayed in the presence of the indicated concentrations of $NaHCO_3$ with 10 mM ATP and 40 mM $MgCl_2$. Data are expressed as nanomoles of cAMP formed per minute per milligram of protein, and values are averages of triplicate determinations. (**B**) Purified sAC_t was assayed as in (A) at the indicated final pHs (buffered by tris-HCl) in the presence (circles) or absence (squares) of 40 mM $NaHCO_3$. Best-fit lines were generated by means of linear regression analysis. (**C**) Engineered soluble tmAC was constructed and purified as described (*19*) and assayed in the presence of $MgCl_2$ alone (basal) or with 50 mM $NaHCO_3$ or 100 μM forskolin. Data are presented as picomoles of cAMP formed per minute per milligram of protein, and values represent triplicate determinations with SDs indicated by error bars.

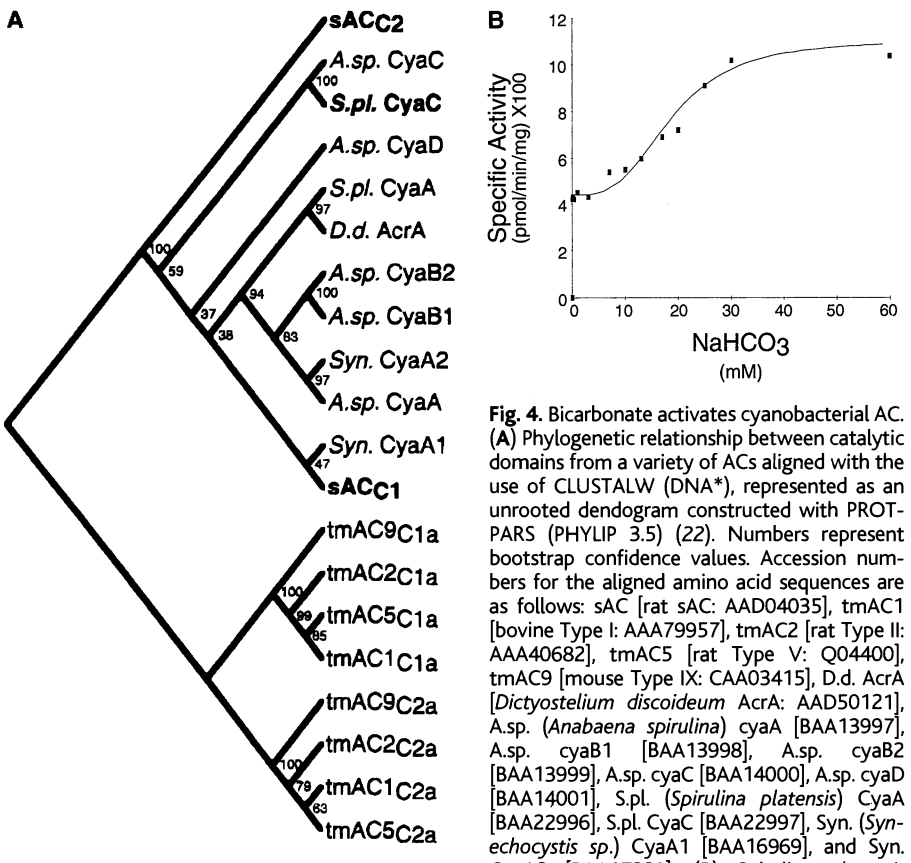

Fig. 4. Bicarbonate activates cyanobacterial AC. (**A**) Phylogenetic relationship between catalytic domains from a variety of ACs aligned with the use of CLUSTALW (DNA*), represented as an unrooted dendogram constructed with PROTPARS (PHYLIP 3.5) (*22*). Numbers represent bootstrap confidence values. Accession numbers for the aligned amino acid sequences are as follows: sAC [rat sAC: AAD04035], tmAC1 [bovine Type I: AAA79957], tmAC2 [rat Type II: AAA40682], tmAC5 [rat Type V: Q04400], tmAC9 [mouse Type IX: CAA03415], D.d. AcrA [*Dictyostelium discoideum* AcrA: AAD50121], A.sp. (*Anabaena spirulina*) cyaA [BAA13997], A.sp. cyaB1 [BAA13998], A.sp. cyaB2 [BAA13999], A.sp. cyaC [BAA14000], A.sp. cyaD [BAA14001], S.pl. (*Spirulina platensis*) CyaA [BAA22996], S.pl. CyaC [BAA22997], Syn. (*Synechocystis sp.*) CyaA1 [BAA16969], and Syn. CyaA2 [BAA17880]. (**B**) *Spirulina platensis* CyaC, expressed and purified as previously described (*23*), was assayed in the presence of the indicated concentrations of $NaHCO_3$ with 100 μM ATP and 5 mM $MnCl_2$ (*23*, *24*). Data are expressed as picomoles of cAMP formed per minute per milligram of protein, and values are averages of triplicate determinations.

for male contraceptives. Furthermore, the expression of mammalian sAC in other bicarbonate-responsive tissues and the evolutionary conservation of bicarbonate-mediated cAMP generation suggest that this signal transduction pathway mediates a wide variety of biological processes.

References and Notes

1. P. E. Visconti *et al.*, *J. Androl.* **19**, 242 (1998).
2. N. B. Garty and Y. Salomon, *FEBS Lett.* **218**, 148 (1987).
3. N. Okamura, Y. Tajima, S. Onoe, Y. Sugita, *J. Biol. Chem.* **266**, 17754 (1991).
4. J. Buck, M. L. Sinclair, L. Schapal, M. J. Cann, L. R. Levin, *Proc. Natl. Acad. Sci. U.S.A.* **96**, 79 (1999).
5. T. Braun, *Methods Enzymol.* **195**, 130 (1991).
6. L. R. Forte, D. B. Bylund, W. L. Zahler, *Mol. Pharmacol.* **24**, 42 (1983).
7. M. L. Sinclair *et al.*, *Mol. Reprod. Dev.* **56**, 6 (2000).
8. Rabbit polyclonal antisera were raised against the catalytic regions of sAC (C1 and C2; amino acids 1 through 469), which were expressed in bacteria and purified from inclusion bodies by excision from SDS–polyacrylamide gel electrophoresis. Antisera were affinity-purified, and specificity was confirmed with heterologously expressed proteins (Fig. 1A). Tissues for Western blotting were purchased from Pel-Freez Biologicals (Rogers, AR). Goat anti-rabbit horseradish peroxidase was used as secondary antibody, and detection was done with enhanced chemiluminescence (Pierce).
9. T. W. Mittag, W. B. Guo, K. Kobayashi, *Am. J. Physiol.* **264**, F1060 (1993).
10. Immunoprecipitations were performed on rat testis cytosol prepared by 100,000*g* centrifugation. Cytosol was incubated with 50 μl of preimmune or anti-sAC antisera for 2 hours at 4°C. After a preclearing spin (for 10 min in a microcentrifuge at full speed), antigen-antibody complexes were harvested by incubation with 60 μl of protein A–Sepharose beads for 1 hour at 4°C. Immunecomplexes were washed twice with 50 mM tris-HCl (pH 7.5) and 100 mM NaCl and were assayed as described (*4*).
11. T. Braun and R. F. Dods, *Proc. Natl. Acad. Sci. U.S.A.* **72**, 1097 (1975).
12. Cellular cAMP accumulation [L. R. Levin and R. R. Reed, *J. Biol. Chem.* **270**, 7573 (1995)] and in vitro AC activity (*4*) in the presence of [α^{32}P]ATP and $MnCl_2$ or $MgCl_2$ (as indicated) were assayed essentially as described. To examine bicarbonate sensitivity of sAC in cellular systems, stable cell lines were starved for bicarbonate (grown in Hepes-buffered, $NaHCO_3$-free Dulbecco's modified Eagle's medium under ambient CO_2) for 24 hours. In vitro AC assays were performed at pH 7.5 in tris-buffered solutions, except where indicated. Kinetic parameters were determined with KinetAsyst II (IntelliKinetics, State College, PA).
13. N. Levine and D. J. Marsh, *J. Physiol.* **213**, 557 (1971).
14. M. J. Cann, unpublished data.
15. M. J. Cann and R. B. Silver, personal communication.
16. sAC_t, which is composed of amino acids 1 through 469, plus a COOH-terminal hexahistidine tag, was heterologously expressed in insect HiFive cells using the Bac-to-Bac Baculovirus Expression System (Life Technologies), and protein was purified by chromatography over Ni^{2+}-NTA Sepharose Resin (Qiagen).
17. R. F. Pitts, *Physiology of the Kidney and Body Fluids* (Year Book Medical Publishers, Chicago, ed. 3, 1974).
18. L. R. Johnson, *Essential Medical Physiology* (Lippincott-Raven, Philadelphia, ed. 2, 1998).

19. K. Scholich, A. J. Barbier, J. B. Mullenix, T. B. Patel, *Proc. Natl. Acad. Sci. U.S.A.* **94**, 2915 (1997).
20. S. Ohno, *J. Mol. Evol.* **44**, S23 (1997).
21. K. Ohmori, M. Hirose, M. Ohmori, *Plant Cell Physiol.* **33**, 21 (1992).
22. J. Felsenstein (Department of Genetics, University of Washington, Seattle, 1993).
23. M. Kasahara, K. Yashiro, T. Sakamoto, M. Ohmori, *Plant Cell Physiol.* **38**, 828 (1997).
24. M. Kasahara and M. Ohmori, *J. Biol. Chem.* **274**, 15167 (1999).
25. We thank R. B. Silver for assistance with in vivo pH measurement; R. Duvoisin, M. C. Gershengorn, C. Nathan, and M. R. Reidenberg for suggestions; J. Qiu for technical assistance; and M. Ohmori for the kind gift of *Spirulina platensis* CyaC in bacterial expression vector. Supported by Weill Medical College of Cornell University Research Associates, the Irma T. Hirschl Trust, The L. W. Frohlich Charitable Trust, Edith C. Blum Foundation, and NIH.

10 March 2000; accepted 23 May 2000

Altered Nociceptive Neuronal Circuits After Neonatal Peripheral Inflammation

M. A. Ruda,* Qing-Dong Ling, Andrea G. Hohmann, Yuan Bo Peng, Toshiya Tachibana

Nociceptive neuronal circuits are formed during embryonic and postnatal times when painful stimuli are normally absent or limited. Today, medical procedures for neonates with health risks can involve tissue injury and pain for which the long-term effects are unknown. To investigate the impact of neonatal tissue injury and pain on development of nociceptive neuronal circuitry, we used an animal model of persistent hind paw peripheral inflammation. We found that, as adults, these animals exhibited spinal neuronal circuits with increased input and segmental changes in nociceptive primary afferent axons and altered responses to sensory stimulation.

Somatosensory development generally requires use-dependent activity during early postnatal times (*1*). However, noxious stimulation is normally absent or infrequent in the neonate. The early neonatal period is a time of great plasticity during which substantia gelatinosa neurons begin to develop their dendritic arbors, c-fibers are functionally immature, and there is as yet limited descending inhibitory modulation of spinal nociceptive neuronal circuits (*2*). The occurrence of persistent inflammation and pain during this period is likely to impact development across several critical time points. Medical procedures used in neonatal intensive care units often involve repeated and lengthy exposure to tissue injury where facial expressions, body movements, and physiological measures suggest a pain response (*3*, *4*) that may alter an individual's response to pain later in life (*5*, *6*).

To produce persistent inflammatory stimulation in newborn rat pups, we injected complete Freund's adjuvant (CFA) into the left hind paw (*7*). The pups exhibited distinct behaviors at the time of CFA injection that imply the presence of pain. These included immediate shaking and licking of the paw and occasional vocalization. The behavioral responses are identical to those seen in adult animal models of pain (*8*). Edema and erythema occurred shortly thereafter and persisted for 5 to 7 days. Injection of saline resulted in paw withdrawal but did not induce the exaggerated shaking or licking of the paw.

Spinal nociceptive neuronal circuits were examined by the selective uptake of wheat germ agglutinin–horseradish peroxidase (WGA-HRP) by a predominantly nociceptive population of unmyelinated and finely myelinated primary afferent axons in the sciatic nerve (*9*). Adult rats that experienced unilateral persistent hind paw inflammation starting on postnatal day one (P1) (n = 10) exhibited ipsilateral increases in the density of WGA-HRP–labeled dorsal horn primary afferents. The increase in laminae I and II labeling was strikingly apparent when afferents from the left and right sciatic nerves were viewed in the same tissue section (Fig. 1, A to D). This side-by-side comparison controlled for possible labeling differences related to animal variability in fixation and timing of the histochemical reaction. Motoneuron labeling, an indicator of comparable sciatic nerve uptake of the tracer, was similar on both sides (see Web fig. 1) (*10*).

Several spinal segments exhibited an increase in density of labeling on the treated as compared with the untreated side. The increase was greatest in caudal segments (Fig. 1, C and D). The most rostral lumbar segments to receive sciatic afferents exhibited the least change in terminal density (Fig. 1A). Quantification (*11*) of the density of WGA-HRP labeling identified a relative increase of 12, 23, and 20% in the L4-5, L5-6, and L6-S1 segments, respectively (Fig. 1E). In addition, a segmental difference in the location of labeled afferents was observed. WGA-HRP–labeled sciatic afferents on the neonatal treated side extended from spinal segments L2 through S1, whereas on the untreated side, these afferents extended from segment L2 only through the juncture of L5 and L6 (Fig. 1F). A similar increase in primary afferent labeling was found in adult rats that received a hind paw CFA injection on either P0 (n = 2) or P3 (n = 3). However, in rats that received a left hind paw CFA injection on postnatal day 14 (P14) (n = 3) (Fig. 2B), the adult distribution of WGA-HRP–labeled sciatic afferents was comparable on the left and right sides of the dorsal horn and did not differ from that of the untreated neonates (Fig. 2A).

To further characterize the population of dorsal root ganglia (DRG) neurons responding to neonatal inflammation (*12*), we used immunohistochemical labeling of the neuropeptide calcitonin gene–related peptide (CGRP) to identify the terminals of neurons that express the nerve growth factor (NGF) receptor, trkA. Isolectin B4 (IB4) binding was used to mark small-diameter DRG neurons that do not express trks (*13*). A distinct increase in staining for CGRP was observed in the dorsal horn on the neonatal treated side (Fig. 2C). No difference was seen in the IB4 labeling pattern on the treated and untreated sides of the spinal cord (Fig. 2D).

β-HRP was used to label nonnociceptive primary afferents that terminated in deeper spinal laminae. The central terminals of sciatic afferents showed comparable labeling of β-HRP on the neonatal treated and untreated side (Fig. 2, E and F) in adult rats that had received a hind paw CFA injection on P1 (n = 5).

The behavioral response to noxious thermal stimuli (*14*) was also studied. Comparable baseline withdrawal latencies were found with the left and right paws of neonatal treated or untreated rats (Fig. 3A). However, 24 hours after a unilateral injection of the inflammatory agent, CFA, into their left hind paws, there was a significant decrease in the paw withdrawal latency in the neonatal treated rats as compared with the untreated rats. Mean latencies were 2.63 ± 0.1 s and 3.13 ± 0.1 s for the treated and untreated groups, respectively (Fig. 3B).

Cellular Neuroscience Section, Pain and Neurosensory Mechanisms Branch, National Institute of Dental and Craniofacial Research, National Institutes of Health (NIH), Bethesda, MD 20892, USA.

*To whom correspondence should be addressed. E-mail: maruda@dir.nidcr.nih.gov